ACS APPLIED MATERIALS & INTERFACES

Research Article

www.acsami.org

Multiple DNA Architectures with the Participation of Inorganic Metal Ions

Guangcheng Wei, Renhao Dong, Xuedong Gao, Dong Wang, Lei Feng, Shasha Song, Shuli Dong, Aixin Song, and Jingcheng Hao*

Key Laboratory for Colloid and Interface Chemistry & Key Laboratory of Special Aggregated Materials, Shandong University, Ministry of Education, Jinan 250100, P.R. China

Supporting Information

ABSTRACT: Here we develop a synthetic protocol for assembling DNA with participating metal ions into multiple shapes. DNA molecules first form coordination complexes with metal ions and these coordination complexes become nucleation sites for primary crystals of metal inorganic salt, and then elementary units of space-filling architectures based on specific geometry form, and finally elementary units assemble into variously larger multiple architectures according to different spatial configurations. We anticipate that our strategy for self-assembling various custom architectures is applicable to most biomolecules possessing donor atoms that can form coordination complexes with metal ions. These multiple architectures provide a general platform for the engineering and assembly of advanced materials possessing features on the micrometer scale and having novel activity.

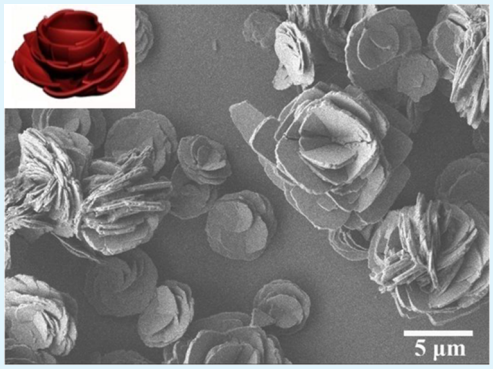

KEYWORDS: *DNA, biomolecules, multiple architectures, metal ions, photocatalysis*

INTRODUCTION

Self-assembly from molecules to multilevel architectures has flourished in recent years; the self-assembly of nucleic acid molecules has shown unique properties for organizing and constructing versatile materials with complex architectures. Among the rich diversity of self-assembled structures, some of the most exquisite architectures were constructed using DNA origami methods;[1−12] however, the DNA origami approach is restricted to discrete domains of complementary strands to link adjacent helices.[13] Herein, a simple method to assemble double-stranded DNA (ds-DNA) via the participation of various metal ions into multidimensional architectures with the aid of anions was developed, the final architecture mainly dependent on the spatial configuration of DNA and biomolecules (chemical structures of biomolecules were described in Figure S1 (see the Supporting Information). We also found that this method (experimental section in the Supporting Information, Figure S2) can be applied to most metal ions and most water-soluble biomolecules having suitable donor atoms. We anticipate that our strategy for self-assembling various architectures based on metal ions and biomolecules will provide a novel and general route to the engineering and assembly of advanced materials.

RESULTS AND DISCUSSION

One dimensional (1D) linear fibers characterize the structures observed in the self-assembly of DNA with Ag^+ ions (Ag^+-DNA system). When appropriate proportions of DNA and Ag^+ in aqueous solution are controlled, 1D linear architectures can be produced (Figures 1 and 2, and Figure S3 in the Supporting Information). With the increase of metal ion portion, the fibers become shorter and wider, and gradually evolve into two-dimensional (2D) planar structures (Figure 2 and Figure S3 in the Supporting Information). For the structure formed by DNA with M^{2+} (e.g., Cu^{2+}, Ca^{2+}, and Co^{2+}), the structures of the

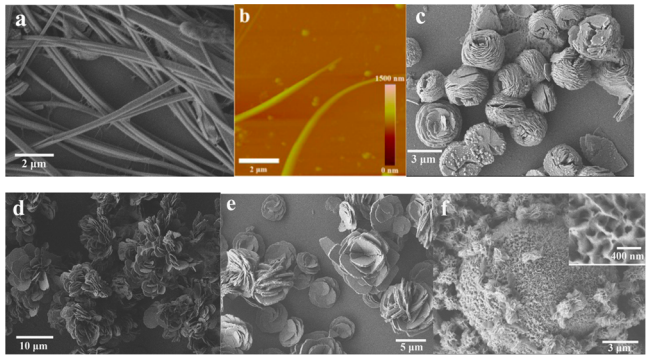

Figure 1. Multiple DNA architectures with different metal ions. (a) SEM and (b) AFM images of Ag^+-DNA (1.0 g L^{-1}) fibers; (c) SEM images of Cu^{2+}-DNA (1.0 g L^{-1}) rosettes and SEM images of Cu^{2+}-DNA microflowers ((d) 0.01 and (e) 0.1 g L^{-1}); (f) SEM images of Ca^{2+}-DNA (0.1 g L^{-1}) tumbleweeds.

Received: April 14, 2014
Accepted: August 18, 2014
Published: August 18, 2014

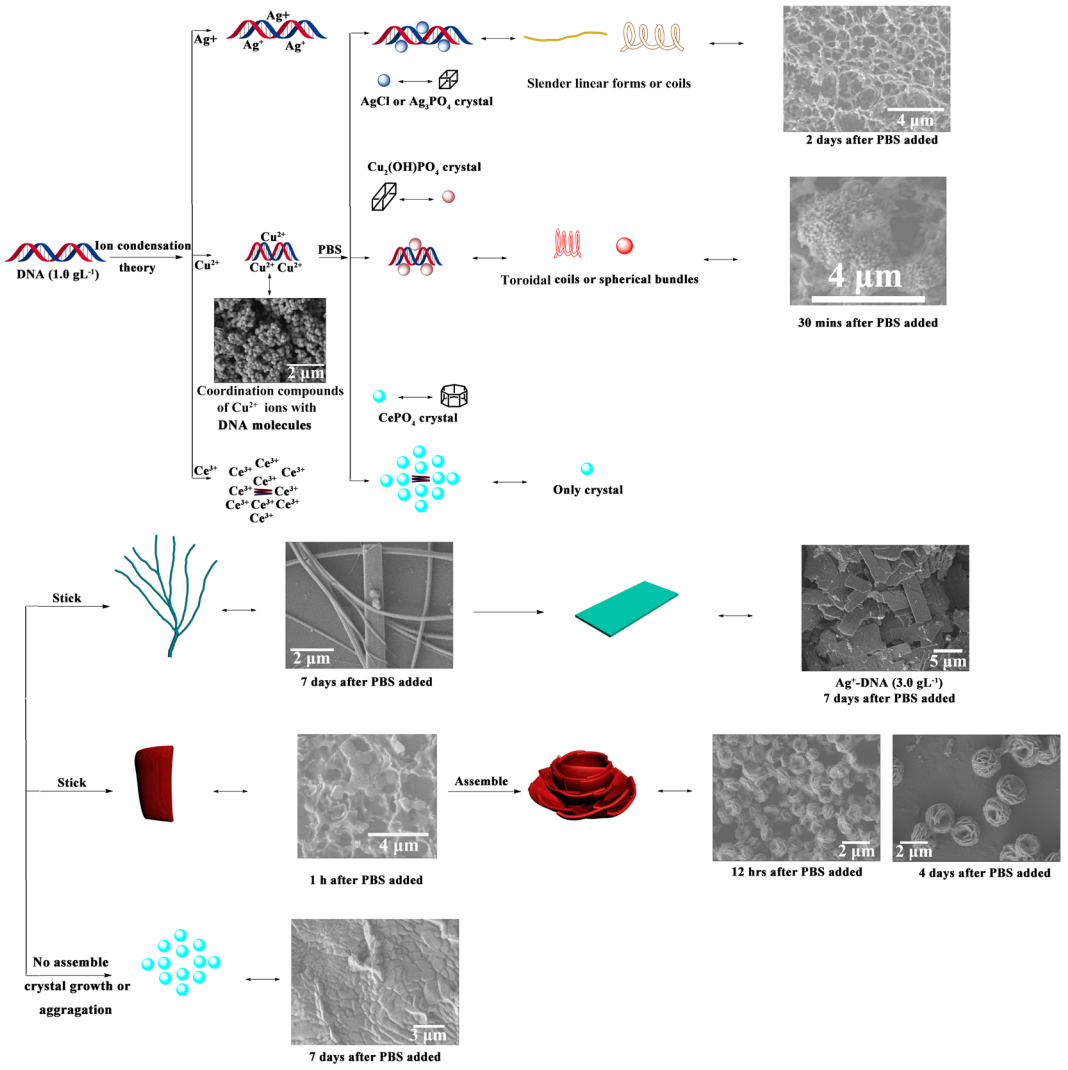

Figure 2. Proposed steps in the formation of multiple architectures arising from DNA condensation with different metal ions which including monovalent metal ion (Ag^+), divalent metal ions (Cu^{2+}) and trivalent metal ions (Ce^{3+}) as shown; all images are SEM images.

main morphology are microflowers (Figures 1, and Figures S4–S6 in the Supporting Information). The elementary unit of microflowers formed in Cu^{2+}-DNA system was sheetlike pedals. With the increase in the proportion between DNA and Cu^{2+}, the pedals of microflowers became smaller and more compact, as shown in Figure 1. The reason may be that with the decrease of DNA amount from 1.0, 0.1 to 0.01 g L^{-1}, the number of nucleation sites decrease, resulting in the rosettes-like structures with larger size.[14] The morphology of the observed structures is microflowers at lower mass ratio of DNA and Cu^{2+} and rosettes at higher mass ratio of DNA and Cu^{2+}, and the final architectures are the result of the assembly of elementary sheet units. For Ca^{2+}-DNA system, hierarchical flower-like structures (tumbleweeds) were typical arising from elementary units of twisted sheets (Figures 1 and Figure S5 in the Supporting Information). No regular architectures were found in the systems formed by DNA with trivalent metal ions such as La^{3+} and Ce^{3+} (see Figure S7 in the Supporting Information).

Neglecting any specific ion-effect, e.g., size, degree of hydration, and coordination preferences, the saturated charge fraction (γ) of DNA by metal ions can be calculated according to ion condensation theory[15−17]

$$\gamma = (1 - (N\xi)^{-1})100\% \quad (1)$$

$$\xi = \frac{q^2}{\varepsilon k \mathrm{Tb}} \quad (2)$$

Where N, ξ, q, ε, k, T, and b are the valence of the counterion, the proportional to the charge density, the charge of the proton, the bulk dielectric constant of solvent, Boltzmann's constant, the temperature (K), and the average helical axial charge spacing, respectively; for water at 25 °C, the value of ξ is $7/b$. The B form of duplex DNA has a step height of 3.4 Å between the base pairs, its b value is 1.7 Å and ξ_{DNA} is 4.2. The monovalent counterions can neutralize the anionic charge of DNA to a maximum value of 76%; for other metal ions the charge can be neutralized 88% for M^{2+}, and 92% for M^{3+}.[16,17]

Intramolecular DNA condensation occurs when the charge is neutralized to more than 89%, and can be induced by M^{2+} ions. Far fewer M^{3+} ions (e.g., one-half to one-fifth) are needed to induce DNA condensation at the same concentration of DNA with mono- and divalent metal ions.[15−17] In our experiments, two kinds of counterions, i.e., Na^+ of DNA and the added metal ions, coexist. Because the concentration of Na^+ is constant, the condensation of DNA is attributed to the added ions. A

transition in the morphology of DNA will occur from the stretched line or coil to toroidal coil or spherical bundles with the condensation proceeding.[15−17] According to the theory of ion induced condensation, the degree of condensation will increase with the increase in the valence of metal ions (Figure 2). A monovalent ion, i.e., Ag^+, cannot induce further compaction of DNA, but the addition of divalent metal ions (e.g., Cu^{2+}, Ca^{2+}, and Co^{2+}) leads to further compaction of DNA to form loose toroids or spherical bundles with a relatively larger radius. In contrast, a small amount of trivalent metal ions (e.g., La^{3+} and Ce^{3+}) condenses DNA to the greatest extent with a spatial configuration of tightly spherical bundles or toroids with smaller radii (Figure 2).

For the Ag^+-DNA system, after adding PBS solution, crystals of insoluble salts, e.g., AgCl and Ag_3PO_4, are adsorbed on the fibers of DNA molecules to form coils or slender linear forms like the spatial configuration of stretched DNA (Figure 2). For the Cu^{2+}-DNA system, the complexes formed by DNA and phosphate salt crystal ($Cu_2(OH)PO_4$) are similar to the spatial configuration of compacted DNA, i.e., toroids or spherical bundles with a relatively larger radius (Figure 2). A small amount of the trivalent ion, Ce^{3+}, can completely condense DNA into spherical shapes with a very small radius. As most Ce^{3+} ions cannot coordinate with DNA, at the early stage of self-assembly, DNA cannot act as the "glue" to associate with the crystals of $CePO_4$ according to specific space geometry, and no regular structures were observed, as shown in Figure 2 and Figure S7 in the Supporting Information. At the medium stage, the elementary units of multiple architectures began to form via the action of DNA acting as a "glue".[14] The elementary units of Ag^+-DNA (1.0 g L^{-1}) system are the linear structure, and those of Cu^{2+}-DNA (1.0 g L^{-1}) system are sheet-like structure (Figure 2). For Ag^+-DNA (1.0 g L^{-1}) system, 1D fibers form and further assemble into 2D sheets if the DNA concentration is large enough (Figure 2). For Cu^{2+}-DNA (1.0 g L^{-1}) system, 2D sheets assemble into a rosette architecture (Figure 2).

For the same valence of metal ions, the final morphology of multiple architectures mainly depended on DNA spatial morphology compressed. One can see that the complexes of Cu^{2+}, Ca^{2+}, and Co^{2+} with DNA have very similar morphology although there is slight difference caused by different spatial morphology compressed of inorganic metal salts and the different coordination modes of metal ions to DNA (Figure 1 and Figure S5 and S6 in the Supporting Information).

The general applicability of this unsophisticated method was further demonstrated by using different biomolecules, an amino acid, small peptides and a protein (Figure 3 and Figures S8−S22 in the Supporting Information) in addition to DNA. The formation of a tetrahedral architecture (Figure 3c) demonstrated the similar mechanism to DNA system, as shown in Figure 3m. The energy-dispersive X-ray microanalysis (EDS) gives direct evidence that all elements existing in the start materials are included in the obtained multiple architectures (see Figures S3−6, S8, and S16 in the Supporting Information). The X-ray diffraction (XRD) patterns showed the highly crystalline state (seeFigures S4, S5, S8 and S16 in the Supporting Information). The same metal ion forms different architectures with different biomolecules, further demonstrating that the spatial morphology compressed of biomolecules and the coordination mode of biomolecules with metal ions play significant role in the formation of multiple architectures.

Interestingly, we also found that the shape and size of glassware affected the morphology of multiple architectures

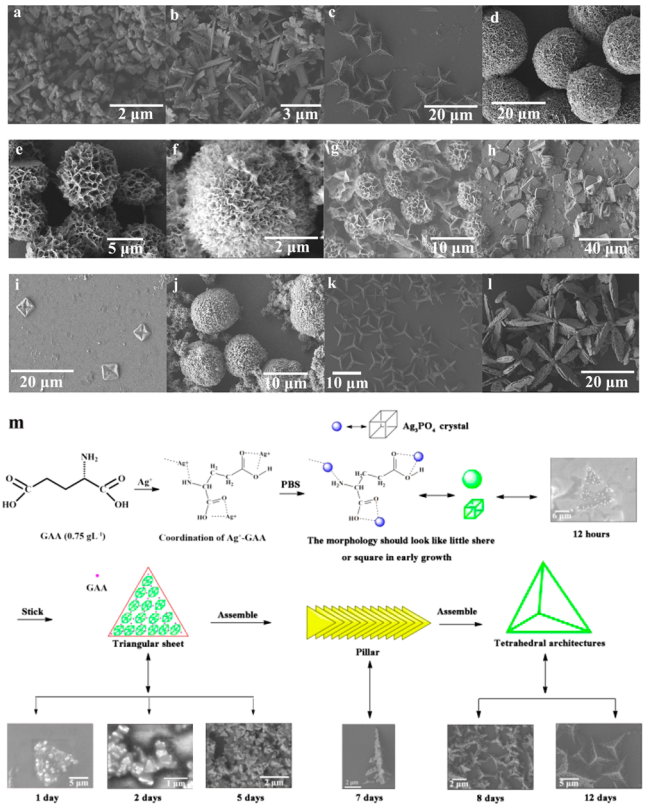

Figure 3. Multidimensional architectures assembled from different metal ions and GAA, GSH and BSA with the aid of phosphate anion. SEM images of Ag^+-GAA architecture ((a) 0.1 g L^{-1}, (b) 0.5 g L^{-1}, and (c) 0.75 g L^{-1}); SEM images of Cu^{2+}-GAA architecture ((d) 0.025 g L^{-1} and (e) 0.5 g L^{-1}); SEM image of Ca^{2+}-GAA ((f) 0.05 g L^{-1}) architecture; SEM image of Cu^{2+}-GSH ((g) 0.1 g L^{-1}) architecture; SEM of Co^{2+}-BSA (0.1 g L^{-1}) architecture (h); SEM of Cd^{2+}-BSA ((i) 1.0 g L^{-1}) architecture; SEM of Ca^{2+}-BSA ((j) 0.01 g L^{-1}) architecture; SEM images of the different morphologies of Ag^+-GAA (0.75 g L^{-1}) systems which were incubated in different glassware: (k) 4 mL of brown serum vial and (l) 500 mL of Erlenmeyer flask; (m) the forming process and mechanism of the tetrahedral architectures.

(Figure 3k, l and Figure S23 in the Supporting Information). We found that a sufficient space in the vessel bottom is needed to accommodate the growth of multiple architectures (see Figure S23 in the Supporting Information). The driving-force during the growth process is affected by the shape and space of the vessel, which induces the different growing directions and self-assembly modes, leading to the multiple structures (Figure 3k, l and Figure S23 in the Supporting Information).

Tetrahedral architectures (Ag^+-GAA (0.75 g L^{-1}) system) and modified tetrahedral architectures ((Ag^+-GAA (0.75 g L^{-1})-AgCl)) were chosen to demonstrate the photocatalytic activity (see Figure S24 in the Supporting Information). The ultraviolet visible diffuse reflectance spectra (UVDLS) reveals that cubic Ag_3PO_4, AgCl crystals, tetrahedral architectures and tetrahedral architectures modified can absorb ultraviolet and visible light as shown in Figure 4a, and the absorbance spectra of tetrahedral architectures modified is more extensive in visible light range, which should be ascribed to the AgCl crystal by the comparison with AgCl UVDLS spectra (Figure 4a). It can be clearly seen that Ag_3PO_4, AgCl, and Ag^+-GAA (0.75 g L^{-1})-AgCl photocatalyst exhibit excellent photocatalytic activities for MO (methyl orange) degradation when ultraviolet light used (Figure 4b). Among them, modified tetrahedral architectures

dx.doi.org/10.1021/am5022667 | ACS Appl. Mater. Interfaces 2014, 6, 14919−14922

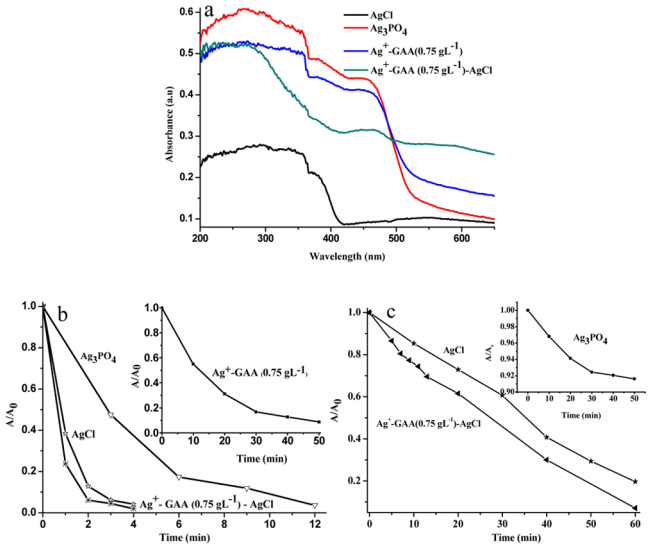

Figure 4. (a) Ultraviolet−visible diffusive reflectance spectra; (b) ultraviolet light irradiation; and (c) visible light irradiation.

exhibit the highest photocatalytic activity and can completely degrade MO dye in only 2 min, which is slightly better than AgCl crystal ,which can completely degrade MO dye in 3, 12, and 50 min to Ag_3PO_4 crystal and tetrahedral architectures separately (Figure 4b). When visible light is used, modified tetrahedral architectures demonstrated excellent photocatalytic activity for MO degradatio. It takes about 60 min, which is slightly better than AgCl crystal as shown in Figure 4c, and the photocatalytic acitivity of Ag_3PO_4 crystal is low among them (Figure 4c). The enhanced activity of modified tetrahedral architectures is probably due to the following reasons: (a) the size of AgCl crystal on tetrahedral architectures is smaller than pure AgCl crystal (see Figure S24 in the Supporting Information), and the smaller crystals possess entirely high energy planes, which should possess great photocatalytic activities;[18] (b) the high surface area of AgCl crystal on the tetrahedral architectures does not lead to significant mass-transfer limitations;[14] (c) synergistic effects of the Ag_3PO_4 crystal among tetrahedral architectures and AgCl crystal. However, the photocatalytic mechanism of modified tetrahedral architectures is notcompletely understood and a more detailed study is still underway.

CONCLUSIONS

In summary, DNA and most water-soluble biomolecules possessing donor atoms (i.e., N and O) can form a variety of novel architectures with most metal ions and with the aid of anions in suitable vessels. We believe that these multiple architectures provide a general platform for the engineering and assembly of advanced materials of biomolecules possessing features on the micrometer scale and having enhanced activity and stability, which might be of great interest for making an attempt on the photocatalyst of the multiple DNA architectures.

ASSOCIATED CONTENT

Supporting Information

Experimental section including chemicals and general preparation methods, TEM and SEM images, EDS and XRD characterizations, and photocatalyst experiments. This material is available free of charge via the Internet at http://pubs.acs.org.

AUTHOR INFORMATION

Corresponding Author

*E-mail: jhao@sdu.edu.cn.

Notes

The authors declare no competing financial interest.

ACKNOWLEDGMENTS

This work was financially supported by the NSFC (21033005 & 21273136).

REFERENCES

(1) Han, D.; Pal, S.; Yang, Y.; Jiang, S.; Nangreave, J.; Liu, Y.; Yan, H. DNA Gridiron Nanostructures Based on Four-Arm Junctions. *Science* **2013**, *339*, 1412−1415.

(2) Sobczak, J. P. J.; Martin, T. G.; Gerling, T.; Dietz, H. Rapid Folding of DNA into Nanoscale Shapes at Constant Temperature. *Science* **2012**, *338*, 1458−1461.

(3) Ke, Y.; Ong, L.; Shih, W.; Yin, P. Three-Dimensional Structures Self-Assembled from DNA Bricks. *Science* **2012**, *338*, 1177−1183.

(4) Kuzyk, A.; Schreiber, R.; Fan, Z.; Pardatscher, G.; Roller, E. M. DNA-Based Self-Assembly of Chiral Plasmonic Nanostructures with Tailored Optical Response. *Nature* **2012**, *483*, 311−314.

(5) Seeman, N. C. DNA in a Material World. *Nature* **2003**, *421*, 427−431.

(6) Winfree, E.; Liu, F.; Wenzler, L. A.; Seeman, N. C. Design and Self-Assembly of Two-Dimensional DNA Crystals. *Nature* **1998**, *394*, 539−544.

(7) Yan, H.; Park, S. H.; Finkelstein, G.; Reif, J. H.; LaBean, T. H. DNA-Templated Self-Assembly of Protein Arrays and Highly Conductive Nanowires. *Science* **2003**, *301*, 1882−1884.

(8) Han, D.; Pal, S.; Nangreave, J.; Deng, Z.; Liu, Y.; Yan, H. DNA Origami with Complex Curvatures in Three-Dimensional Space. *Science* **2011**, *332*, 342−346.

(9) Douglas, S. M.; Dietz, H.; Liedl, T.; Högberg, B.; Graf, F.; Shih, W. M. Self-Assembly of DNA into Nanoscale Three-Dimensional Shapes. *Nature* **2009**, *459*, 414−418.

(10) Martin, T. G.; Dietz, H. Magnesium-Free Self-Assembly of Multi-Layer DNA Objects. *Nat. Commun.* **2012**, *3*, 1103−1108.

(11) Fu, Y.; Zeng, D.; Chao, J.; Jin, Y.; Zhang, Z.; Liu, H.; Li, D.; Ma, H.; Huang, Q.; Gothelf, K. V.; Fan, C. Single-Step Rapid Assembly of DNA Origami Nanostructures for Addressable Nanoscale Bioreactors. *J. Am. Chem. Soc.* **2013**, *135*, 696−702.

(12) Zhang, C.; Tian, C.; Guo, F.; Liu, Z.; Jiang, W.; Mao, C. DNA-Directed Three-Dimensional Protein Organization. *Angew. Chem., Int. Ed.* **2012**, *51*, 3382−3385.

(13) Rothemund, P. W. K. DNA-Directed Three-Dimensional Protein Organization. *Nature* **2006**, *440*, 297−302.

(14) Ge, J.; Lei, J.; Zare, R. N. Protein−Inorganic Hybrid Nanoflowers. *Nat. Nanotechnol.* **2012**, *7*, 428−432.

(15) Widom, J.; Baldwin, R. L. Cation-Induced Toroidal Condensation of DNA Studies with $Co^{3+}(NH_3)_6$. *J. Mol. Biol.* **1980**, *144*, 431−453.

(16) Manning, G. S. The Molecular Theory of Polyelectrolyte Solutions with Applications to the Electrostatic Properties of Polynucleotides. *Q. Rev. Biophys.* **1978**, *2*, 179−246.

(17) Wilson, R. W.; Bloomfield, V. A. Counterion-Induced Condensation of Deoxyribonucleic acid. A Light-Scattering Study. *Biochemistry* **1979**, *18*, 2192−2196.

(18) Bi, Y.; Ouyang, S.; Umezawa, N.; Cao, J.; Ye, J. Facet Effect of Single-Crystalline Ag_3PO_4 Sub-microcrystals on Photocatalytic Properties. *J. Am. Chem. Soc.* **2011**, *133*, 6490−6492.